2001

Spatial Symmetry Breaking in the Belousov-Zhabotinsky Reaction with Light-Induced Remote Communication

M. Hildebrand

H. Skødt

K. Showalter

Spatial Symmetry Breaking in the Belousov-Zhabotinsky Reaction with Light-Induced Remote Communication

M. Hildebrand,[1,2] H. Skødt,[1] and K. Showalter[1,2]

[1]*Department of Chemistry, West Virginia University, Morgantown, West Virginia 26506-6045*
[2]*Fritz-Haber-Institut der Max-Planck-Gesellschaft, Faradayweg 4-6, D-14195 Berlin, Germany*

(Received 18 December 2000; revised manuscript received 2 May 2001; published 6 August 2001)

Domains containing spiral waves form on a stationary background in a photosensitive Belousov-Zhabotinsky reaction with light-induced alternating nonlocal feedback. Complex behavior of colliding and splitting wave fragments is found with feedback radii comparable to the spiral wavelength. A linear stability analysis of the uniform stationary states in an Oregonator model reveals a spatial symmetry breaking instability. Numerical simulations show behavior in agreement with that found experimentally and also predict a variety of other new patterns.

DOI: 10.1103/PhysRevLett.87.088303 PACS numbers: 82.40.Ck, 05.65.+b, 47.54.+r, 82.30.Vy

Physicochemical systems with coupled processes on different length scales often exhibit stationary spatially periodic structures arising from symmetry breaking instabilities [1–3]. In nonequilibrium systems, such structures occur in activator-inhibitor systems with short-range activation and long-range inhibition [1], while in equilibrium systems they arise from the competition of short-range attractive interactions and long-range repulsion [2]. Recent investigations also revealed spatial symmetry breaking arising from the interplay between short-range attractive interactions and a long-range reaction-diffusion process [3]. In this Letter, we report on novel spatiotemporal patterns in the photosensitive Belousov-Zhabotinsky (BZ) reaction [4] arising from a nonlocal feedback that imposes short-range activation and long-range inhibition.

The photosensitive BZ reaction has proven to be an ideal model system for studies of perturbed excitable media. The medium excitability can be precisely controlled by exposure to 460 nm light, enabling the application of a wide variety of external perturbations. Entrainment of spiral wave meandering [5] and the formation of labyrinthine patterns [6] have been found with periodic forcing. Resonance attractors [7] and oscillatory cluster patterns [8] were recently reported in photosensitive BZ systems with different types of global feedback.

We study the photosensitive BZ reaction with nonlocal coupling over a wide range of length scales, from much larger than the characteristic reaction-diffusion length scale to length scales that are comparable. The kernel of the feedback alternates from positive (activatory) for short distances to negative (inhibitory) for larger distances. We show below that such a feedback gives rise to a "Turing-like" instability, and, as a result, patterns with more than one characteristic length scale are formed.

Experiments were carried out with the catalyst of the light-sensitive BZ reaction, $Ru(bpy)_3^{2+}$, immobilized in a thin slab of silica gel. The gel was continuously fed with a fresh, catalyst-free BZ solution in a reactor thermostated at 23.0 °C to maintain constant, nonequilibrium conditions [9]. The silica gel medium was prepared by acidifying a solution of 10% (w/w) Na_2SiO_3 and 2.0 mM $Ru(bpy)_3^{2+}$ with H_2SO_4 and by casting a uniform $0.3 \times 20.0 \times 25.6$ mm^3 layer onto a microscope slide.

Prior to each experiment, the projected image was adjusted at each pixel by an iterative algorithm to ensure a spatially uniform illumination field [6,10]. The local concentration of oxidized catalyst was recorded with a CCD-camera, and the recorded image was divided into an array of 100×128 square cells. In all of our experiments, the lateral size of each cell was much smaller than the spiral wavelength. The nonlocal feedback occurred via an illumination field (2.5×2.0 cm^2) projected from a computer-controlled video projector onto the face of the gel medium through a 460 nm bandpass filter. The feedback was updated at 2 s intervals. Bromide ions were locally produced in a photochemical cycle, and, as a result, the local excitability was appropriately modified by the feedback signal [11].

The intensity $I(\mathbf{r}, t)$ of the projected illumination field was computed as

$$I(\mathbf{r}, t) = \frac{I_{\max}}{2}\{1 - \tanh[\chi V(\mathbf{r})]\}, \qquad (1)$$

where $I_{\max}$ (approximately 80 mW/cm^2) is the maximum light intensity, the parameter χ characterizes the width of the interface in which I increases from zero to $I_{\max}$, and $V(\mathbf{r}) = \sum w(\mathbf{r} - \mathbf{r}')v(\mathbf{r}')$ represents the coarse grained effective nonlocal potential, which depends linearly on the concentration of the oxidized catalyst, v, in the neighborhood of point $\mathbf{r}$. The summation over $\mathbf{r}'$ extends over the entire array of square cells [12]. The kernel $w(\mathbf{r})$ represents an "effective binary potential" (cf. [13]) for the oxidized catalyst. Here, we choose

$$w(\mathbf{r}) = \frac{1}{\pi r_2^2}\exp\left(-\frac{r^2}{r_2^2}\right) - \frac{1}{\pi r_1^2}\exp\left(-\frac{r^2}{r_1^2}\right), \qquad (2)$$

with $r_1 > r_2$, i.e., $w(\mathbf{r})$ is positive for short distances r and negative for larger distances. If the characteristic radii r_1

and r_2 are chosen sufficiently larger than the spiral wavelength, a labyrinthine pattern of domains containing spiral waves is exhibited on a stationary background, for both excitable [Figs. 1(a) and 1(b)] and oscillatory [Figs. 1(c) and 1(d)] conditions. After an initial transient, the boundaries of the spiral domains remain stationary, as can be seen by comparing panels 1(a) and 1(b) or 1(c) and 1(d). Note that the domains containing spiral waves and the domains with a stationary catalyst concentration become larger as the characteristic radii r_1 and r_2 are increased. As the radii are decreased and the characteristic size of the spiral domains becomes comparable to the spiral wavelength, wave propagation is completely suppressed for excitable conditions. Under oscillatory conditions, however, we find complex behavior with traveling wave fragments that interact and split as they reach a critical size [see Figs. 1(e) and 1(f)].

Wave propagation in the light-sensitive ruthenium-catalyzed BZ reaction can be simulated with a modified two-variable Oregonator model [14] that includes a term

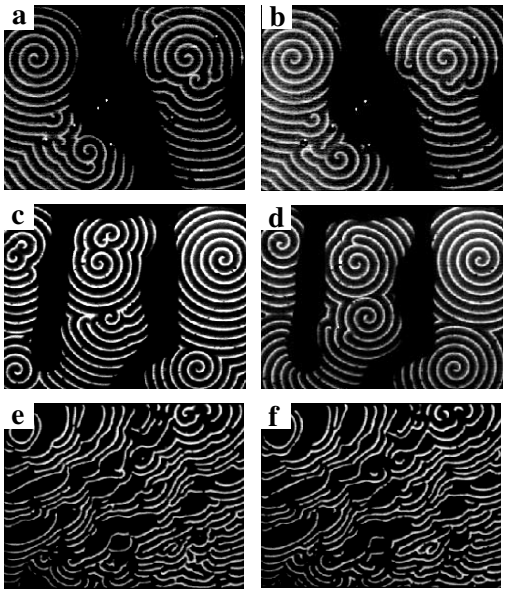

FIG. 1. (a)–(d): Formation of spiral domain patterns on a stationary background in the BZ reaction with light-induced nonlocal feedback given by Eq. (1). Snapshots (a) and (b) show behavior in an excitable medium (in the absence of feedback), with (b) recorded 30 min after (a), while (c) and (d) correspond to an oscillatory medium (in the absence of feedback), with (d) recorded 30 min after (c). The gray level is proportional to the concentration of $\mathrm{Ru}(bpy)_3^{3+}$, increasing from black to white. The recorded image was divided into an array of 100×128 square cells, with $r_1 = 28$, $r_2 = 14$ pixels in (a), (b) and $r_1 = 14$, $r_2 = 7$ pixels in (c), (d). The composition of the catalyst-free BZ reaction mixture was: $0.28M$ BrO_3^-, $0.175M$ malonic acid, $0.15M$ bromomalonic acid, and $0.4M$ H_2SO_4 in (a) and (b), and $0.5M$ BrO_3^-, $0.125M$ malonic acid, $0.125M$ bromomalonic acid, and $0.25M$ H_2SO_4 in (c) and (d). The behavior with the coupling length scale comparable to the spiral wavelength ($r_1 = 4$, $r_2 = 2$ pixels) is shown in (e) and (f), with (f) recorded 8 s after (e) and all other parameters as in (c) and (d).

$\phi = \phi(\mathbf{r}, t)$ to account for the photochemically produced bromide during external illumination of the system [15]:

$$\frac{\partial u}{\partial t} = \nabla^2 u + \frac{1}{\varepsilon}\left\{u - u^2 - [fv + \phi(\mathbf{r}, t)]\frac{u - q}{u + q}\right\},$$

$$\frac{\partial v}{\partial t} = u - v, \tag{3}$$

where the variables u and v correspond to the concentrations of the autocatalytic species $HBrO_2$ and the oxidized catalyst $\mathrm{Ru}(bpy)_3^{3+}$, respectively; ε and q are scaling parameters and f is an adjustable stoichiometry parameter. The rate of bromide production from irradiation ϕ is proportional to the light intensity $I(\mathbf{r}, t)$, as given by Eq. (1) (with the proportionality factor $K/I_{\max}$) . In most of the simulations we used $V(\mathbf{r}) = \int w(\mathbf{r} - \mathbf{r}')v(\mathbf{r}')\,d\mathbf{r}'$ instead of the coarse grained version described above. Note that $\phi(\mathbf{r}, t) \to KH[-V(\mathbf{r}, t)]$ as $\chi \to \infty$, where $H(z) = 1$ for $z \geq 0$ and $H(z) = 0$ for $z < 0$.

In the infinite system, the stationary uniform states of Eqs. (3) satisfy $u = v = u_0$, where u_0 is obtained as a solution of the cubic equation $u^3 - (1 - q - f)u^2 - (q + qf - K/2)u - qK/2 = 0$. If f is sufficiently large, this equation has a single solution. It can be either stable or unstable with respect to uniform perturbations. Moreover, the stability of the uniform stationary state can be tested in the one-dimensional system by adding small spatially periodic perturbations with wave number k and linearizing Eqs. (3). The elements of the corresponding Jacobian are given by $J_{11}(k) = \varepsilon^{-1}[1 - 2u_0 - 2q(fu_0 + K/2)/(u_0 + q)^2] - k^2$, $J_{12}(k) = -\varepsilon^{-1}(u_0 - q)\{f + K\chi[\exp(-r_1^2k^2/4) - \exp(-r_2^2k^2/4)]/2\}/(u_0 + q)$, $J_{21}(k) = 1$, and $J_{22}(k) = -1$. The eigenvalues $\gamma_k^{\pm}$ are given by $2\gamma_k^{\pm} = [J_{11}(k) - 1] \pm \{[J_{11}(k) - 1]^2 + 4[J_{11}(k) + J_{12}(k)]\}^{1/2}$. It can be readily shown that unstable modes with nonzero wave numbers always have real growth rates. Hence, the instability is analogous to the classic Turing bifurcation in activator-inhibitor systems [1]: The dispersion $\mathrm{Re}[\gamma_k^+]$ has a single maximum at a wave number k_0, which changes its sign at the instability. Here, the conditions determining k_0 and the instability boundaries correspond to the equations $B_k \equiv J_{11}(k) + J_{12}(k) = 0$ and $\partial B_k/\partial k^2 = 0$, which can be satisfied *if* $r_1 > r_2$ *and* χ *is sufficiently large.* We note that this type of instability can also be found if $\phi(\mathbf{r}, t)$ depends linearly on V. In this case, however, the proportionality factor K must be unrealistically high (typically larger than 1).

Typical dispersion relations $\mathrm{Re}(\gamma_k^+)$ in the vicinity of the symmetry breaking instability are shown in Fig. 2(a): The dispersion exhibits a single maximum for $\chi = 550$, but all growth rates are negative. The maximum of γ_k^+ changes sign at the critical value $\chi = 590$, and, for $\chi = 630$, perturbations grow for a wide interval of wave numbers.

Figure 2(b) shows the stability boundaries of the homogeneous stationary state in the parameter plane (f, χ)

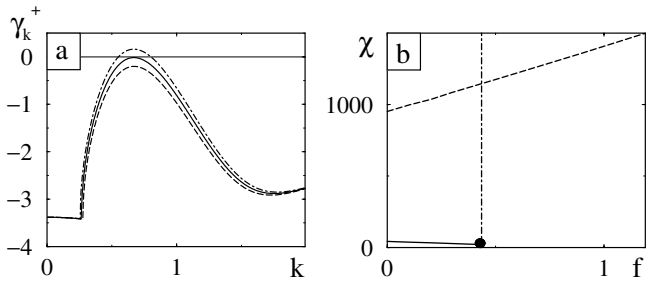

FIG. 2. (a) Dispersion relations $\mathrm{Re}[\gamma_k^+]$ vs k for the reduced uniform stationary state in model (3). Parameters are $\varepsilon = 0.05$, $f = 1.9$, $q = 0.005$, $r_1 = 4$, $r_2 = 2$, $K = 0.02$, and $\chi = 550$ (dashed line), $\chi = 590$ (solid line), and $\chi = 630$ (dot-dashed line). (b) Bifurcation diagram for uniform stationary states in the parameter plane (f, χ) for $\varepsilon = 0.05$, $q = 0.005$, $r_1 = 4$, $r_2 = 2$, and $K = 0.1$. The solid and dot-dashed lines mark the symmetry breaking instability and Hopf bifurcation of the oxidized stationary state, respectively. The dashed line corresponds to the symmetry breaking instability of the reduced stationary state. The black circle denotes the codimension-2 point (see text).

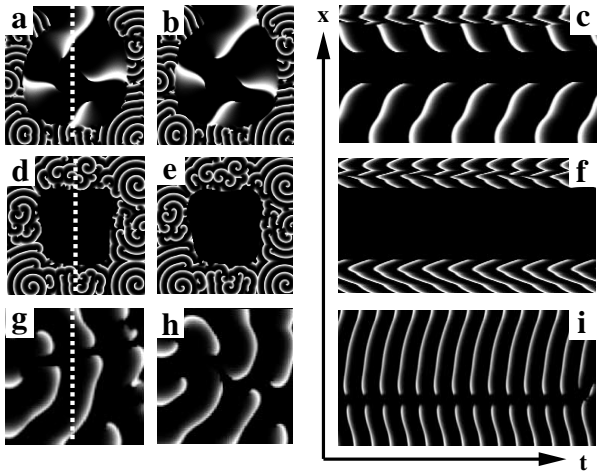

FIG. 3. Two-dimensional evolution of the oxidized catalyst concentration, $v(x, y)$ (increasing from black to white), in Eqs. (3) for large f. The temporal evolution in the one-dimensional cross sections indicated by the dashed white lines in (a), (d), and (g) is shown in (c), (f), and (i) during time T; successive snapshots are separated by Δt, and the nonlocal term [ϕ in Eq. (1)] is updated at intervals of t_{up}. The parameters, $q = 0.005$, $\varepsilon = 0.05$, $f = 1.9$, $\chi = 22\,000$, and $K = 0.1$, and no-flux boundary conditions were used for u and $v = 0$ outside the medium. Other parameters are as follows. (a)–(c): $r_1 = 50$, $r_2 = 25$, system size $L = 256$, $\Delta t = T = 31.3$, and $t_{\mathrm{up}} = 0.03125$. (d)–(f): $r_1 = 50$, $r_2 = 25$, $L = 256$, $\Delta t = T = 31.3$, and $t_{\mathrm{up}} = 0.625$. (g)–(i): $r_1 = 4$, $r_2 = 2$, $L = 50$, $\Delta t = T = 62.5$, and $t_{\mathrm{up}} = 0.0016$. The lattice spacing was $dx = 0.25$ and the time step $dt = 1.6 \times 10^{-4}$; V was calculated on a coarse grained lattice with spacing $4dx$.

for $K = 0.1$. For all values of f, a homogeneous steady state solution of Eqs. (3) exists with a low concentration v (the reduced steady state), which is always stable with respect to homogeneous perturbations. For $f < 0.592$, this state coexists with another uniform stationary state with a relatively high concentration of v (the oxidized steady state). The latter undergoes a subcritical Hopf bifurcation at $f = 0.435$ (dot-dashed line) and is stable with respect to uniform perturbations for $f < 0.435$. A spatial symmetry breaking instability occurs as χ reaches threshold values for both the reduced (dashed line) and oxidized (solid line) stationary states. The Hopf bifurcation and the Turing-like instability of the oxidized stationary state meet in a codimension-2 point (shown by the black dot). This situation is similar to the classical Turing-Hopf bifurcation that has been analyzed in reaction-diffusion systems (e.g., in [16]). In the case of Fig. 2(b), however, both the temporal and spatial bifurcations are subcritical.

We have carried out numerical simulations with Eqs. (3) in the parameter regions corresponding to the experiments shown in Fig. 1. For sufficiently large values of the characteristic interaction radii, spiral domains [Figs. 3(a)–3(f)] are formed. The boundaries of these domains do not significantly change in the course of the simulations. The behavior depends on the rate at which the nonlocal term ϕ in Eq. (1) is updated. When ϕ is updated at short time intervals, wave fragments are periodically generated at the spiral domain boundaries. These waves, which have a much larger wavelength than the spiral waves within the domains, travel into the predominantly reduced regions until they are annihilated, typically by collisions with the boundaries of nearby spiral domains [Figs. 3(a)–3(c)]. When ϕ is updated at larger time intervals (but still smaller than the spiral period $T_S \approx 3.15$), these traveling wave fragments are suppressed [Figs. 3(d)–3(f)], i.e., the spiral domains form on a stationary background as in the experiments [Figs. 1(a)–1(d)]. Note that here the spiral domains form preferably at the boundaries of the medium as a consequence of the Dirichlet boundary conditions for v [12]. The fact that we do not find mixed patterns as shown in Figs. 3(a)–3(c) in our experiments suggests that the minimal experimental time between updates of 2 s is already too large for these patterns to exist.

If the characteristic radii of the feedback are smaller than the spiral wavelength and the medium is oscillatory, we find complex dynamics of wave fragments that collide or split [Figs. 3(g)–3(i)], as in the experiments for oscillatory conditions [cf. Figs. 1(e) and 1(f)]. In the excitable regime for small interaction radii, stationary structures with extremely small amplitudes are formed. Such structures would be difficult to detect experimentally, which is consistent with our observation of a seemingly homogeneous stationary state for these conditions in the experiments.

Simulations with Eqs. (3) were also carried out in the parameter region that lies to the left of the codimension-2 point shown in Fig. 2(b). There, the reduced and oxidized stationary states coexist and the system is excitable with respect to the oxidized stationary state in the absence of illumination. For small radii, we find the formation of stationary spatially periodic structures with significant amplitudes [Figs. 4(a)–4(c)] or oscillating domain patterns [Figs. 4(d)–4(f)]. Figures 4(g)–4(i) show a simulation for

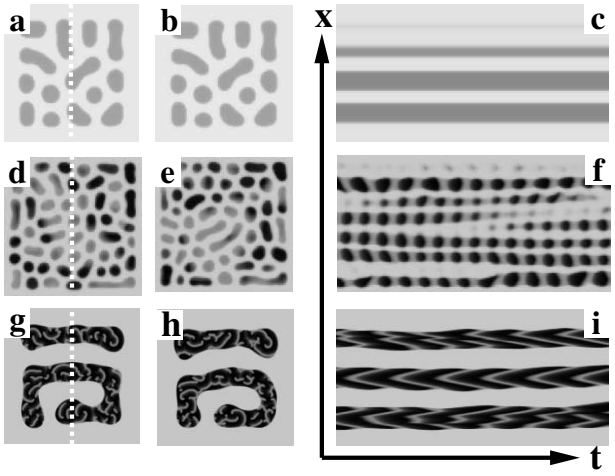

FIG. 4. The two-dimensional evolution of the oxidized catalyst concentration, $v(x, y)$, in Eqs. (3) for small f, $q = 0.005$, $\varepsilon = 0.05$, and $K = 0.1$. Notations and numerical parameters are the same as in Fig. 3, with the following other parameters. (a)–(c): $f = 0.25$, $r_1 = 4$, $r_2 = 2$, $\chi = 2500$, $L = 50$, $\Delta t = 305$, $t_{\text{up}} = 1.6 \times 10^{-4}$, and $T = 101.6$. (d)–(f): $r_1 = 4$, $r_2 = 2$, $\chi = 2000$, $f = 0.37$, $L = 50$, $\Delta t = 62.5$, $t_{\text{up}} = 0.0016$, and $T = 62.5$. (g)–(i): $f = 0.37$, $r_1 = 25$, $r_2 = 12.5$, $\chi = 2400$, $L = 200$, $\Delta t = 62.5$, $t_{\text{up}} = 0.0016$, and $T = 31.3$.

large radii under such conditions. We now observe the formation of spiral domains on a stationary background corresponding to the oxidized stationary state (gray area). Inside the domains, spirals with an increased concentration of oxidized catalyst form on a background with predominantly reduced catalyst (black shaded regions). Future experimental studies will examine this parameter regime in order to search for the types of behavior shown in Fig. 4 [17]. We note that the patterns shown in Figs. 3 and 4 are generally observed in the Turing-unstable region as long as the intensity of the feedback K is high enough. For smaller values of K, however, codimension-2 points can also be found for the reduced stationary state [17].

In summary, we have shown that nonlocal feedback in an active system gives rise to the emergence of new patterns characterized by multiple length scales which result from the interaction of a symmetry breaking instability with excitable or oscillatory local kinetics. We note that this mechanism for the formation of complex domain patterns might play a role in biological systems, such as neural tissues with nonlocal coupling. We also point out that the evolution equation (3) with an effective binary potential similar to Eq. (2) can be derived as a limiting case of a four-variable reaction-diffusion system [17].

We thank E. Mihaliuk for help with the experimental setup. M. H. was supported by the A. von Humboldt foundation and H. S. was supported by the Danish Research Academy. K. S. thanks the National Science Foundation (Grant No. CHE-9974336) and the Office of Naval Research for supporting this research.

[1] A. M. Turing, Philos. Trans. R. Soc. London B **237**, 37 (1952); V. Castets, E. Dulos, J. Boissonade, and P. De Kepper, Phys. Rev. Lett. **64**, 2953 (1990).
[2] M. Seul and D. Andelman, Science **267**, 476 (1995), and references therein.
[3] S. C. Glotzer, E. A. Di Marzio, and M. Muthukumar, Phys. Rev. Lett. **74**, 2034 (1995); Q. Tran-Cong, J. Kawai, and K. Endoh, Chaos **9**, 298 (1999); M. Hildebrand, A. S. Mikhailov, and G. Ertl, Phys. Rev. E **58**, 5483 (1998).
[4] A. N. Zaikin and A. M. Zhabotinsky, Nature (London) **225**, 535 (1970); V. Gáspár, G. Bazsa, and M. T. Beck, Z. Phys. Chem. (Leipzig) **264**, 43 (1983); L. Kuhnert, Nature (London) **319**, 393 (1986).
[5] O. Steinbock, V. S. Zykov, and S. C. Müller, Nature (London) **366**, 322 (1993).
[6] V. Petrov, Q. Ouyang, and H. L. Swinney, Nature (London) **388**, 655 (1997); A. L. Lin, A. Hagberg, A. Ardelea, M. Bertram, H. L. Swinney, and E. Meron, Phys. Rev. E **62**, 3790 (2000).
[7] S. Grill, V. S. Zykov, and S. C. Müller, Phys. Rev. Lett. **75**, 3368 (1995).
[8] V. K. Vanag, L. Yang, M. Dolnik, A. M. Zhabotinsky, and I. R. Epstein, Nature (London) **406**, 389 (2000).
[9] Z. Noszticzius, W. Horsthemke, W. D. McCormick, H. L. Swinney, and W. Y. Tam, Nature (London) **329**, 619 (1987).
[10] S. Kádár, J. Wang, and K. Showalter, Nature (London) **391**, 770 (1998).
[11] S. Kádár, T. Amemiya, and K. Showalter, J. Phys. Chem. **101**, 8200 (1997).
[12] Throughout this Letter we apply Dirichlet boundary conditions for v setting $v = 0$ outside the medium. Control experiments with Neumann and periodic boundary conditions for v reveal no qualitative differences in behavior.
[13] M. Hildebrand and A. S. Mikhailov, J. Phys. Chem. **100**, 19 089 (1996).
[14] R. J. Field and R. M. Noyes, J. Chem. Phys. **60**, 1877 (1974); J. J. Tyson and P. C. Fife, J. Chem. Phys. **73**, 2224 (1980).
[15] H. J. Krug, L. Pohlmann, and L. Kuhnert, J. Phys. Chem. **94**, 4862 (1990).
[16] A. De Wit, D. Lima, G. Dewel, and P. Borckmans, Phys. Rev. E **54**, 261 (1996).
[17] H. Skødt, M. Hildebrand, and K. Showalter (to be published).